Single-molecule visualization of Saccharomyces cerevisiae leading-strand synthesis reveals dynamic interaction between MTC and the replisome

Lewis, Jacob S.; Spenkelink, Lisanne M.; Schauer, Grant D.; Hill, Flynn R.; Georgescu, Roxanna E.; O'Donnell, Michael E.; van Oijen, Antoine M.

Published in:
Proceedings of the National Academy of Sciences of the United States of America

DOI:
10.1073/pnas.1711291114

Publication date:
2017

Single-molecule visualization of *Saccharomyces cerevisiae* leading-strand synthesis reveals dynamic interaction between MTC and the replisome

Jacob S. Lewis[a,b,1], Lisanne M. Spenkelink[a,b,c,1], Grant D. Schauer[d], Flynn R. Hill[a,b], Roxanna E. Georgescu[d], Michael E. O'Donnell[d,2], and Antoine M. van Oijen[a,b,2]

[a]Centre for Medical & Molecular Bioscience, University of Wollongong, Wollongong, NSW 2522, Australia; [b]Illawarra Health & Medical Research Institute, Wollongong, NSW 2522, Australia; [c]Zernike Institute for Advanced Materials, University of Groningen, 9747 AG Groningen, The Netherlands; and [d]Howard Hughes Medical Institute, Rockefeller University, New York, NY 10065

Contributed by Michael E. O'Donnell, August 24, 2017 (sent for review June 23, 2017; reviewed by David Rueda and Michael Trakselis)

The replisome, the multiprotein system responsible for genome duplication, is a highly dynamic complex displaying a large number of different enzyme activities. Recently, the *Saccharomyces cerevisiae* minimal replication reaction has been successfully reconstituted in vitro. This provided an opportunity to uncover the enzymatic activities of many of the components in a eukaryotic system. Their dynamic behavior and interactions in the context of the replisome, however, remain unclear. We use a tethered-bead assay to provide real-time visualization of leading-strand synthesis by the *S. cerevisiae* replisome at the single-molecule level. The minimal reconstituted leading-strand replisome requires 24 proteins, forming the CMG helicase, the Pol ε DNA polymerase, the RFC clamp loader, the PCNA sliding clamp, and the RPA single-stranded DNA binding protein. We observe rates and product lengths similar to those obtained from ensemble biochemical experiments. At the single-molecule level, we probe the behavior of two components of the replication progression complex and characterize their interaction with active leading-strand replisomes. The Mini-chromosome maintenance protein 10 (Mcm10), an important player in CMG activation, increases the number of productive replication events in our assay. Furthermore, we show that the fork protection complex Mrc1–Tof1–Csm3 (MTC) enhances the rate of the leading-strand replisome threefold. The introduction of periods of fast replication by MTC leads to an average rate enhancement of a factor of 2, similar to observations in cellular studies. We observe that the MTC complex acts in a dynamic fashion with the moving replisome, leading to alternating phases of slow and fast replication.

DNA replication | single-molecule biophysics | replisome | CMG | Mrc1

The replisome is the molecular machine that coordinates the enzymatic activities required for genome duplication. It contains proteins responsible for DNA unwinding, depositing primers, synthesizing DNA, and coordinating DNA production on both strands. The replisome in eukaryotes is a sophisticated and highly regulated machine; its assembly is performed by origin-initiation proteins and kinases that restrict chromosome duplication to a single round to ensure proper ploidy across multiple chromosomes. Replisome operations must be finely tuned to adjust to changing cellular conditions and to interface with numerous repair pathways. While the minimal operating machinery to advance a replication fork has been established in vitro (1, 2), the reactions were unable to achieve rates measured in vivo. This deficiency is not surprising considering the several additional proteins that move with replisomes in vivo (3, 4). The evolution of checkpoints has provided eukaryotic cells with surveillance mechanisms that orchestrate the recruitment of many other proteins to replication forks that modulate replisome activity. Using simplified in vitro assays, study of these additional proteins has resulted in the reconstitution of efficient leading- and lagging-strand DNA replication on naked and chromatinized templates in vitro (1, 3–7).

Once CMG helicase and the Pol ε leading-strand DNA polymerase (together called CMGE) are assembled at the replication fork, additional proteins are conscripted to the complex to form the RPC. These proteins include Ctf4, Csm3, FACT, Mrc1, Pol α, Tof1, and Top1 (8). It has been shown that Mrc1, a yeast homolog of Claspin and an S-phase-specific mediator protein of the DNA damage response, is recruited to the fork (8, 9) and increases the rate of replication in vivo about twofold (10–12). In vitro studies confirm that Mrc1 increases the speed of replication forks to rates similar to those measured in vivo (5). Inclusion of Csm3/Tolf1 stimulated the functional association of Mrc1 with the replisome. Mrc1 binds both the N- and C-terminal halves of Pol2, the polymerase/exonuclease of Pol ε (13). Given that we have only begun to determine the exact roles of the individual proteins at the fork, understanding basic mechanisms during DNA replication that coordinate enzymatic activity has thus far been very challenging. To date, all in vitro methods used to study *Saccharomyces cerevisiae* DNA replisome activity have relied on traditional biochemical techniques (1–5, 7). Such experiments have provided the molecular mechanisms that target the replicative polymerases to their respective strands during bulk DNA synthesis (1–3, 14). However, these ensemble methods only report averages of total DNA synthesis. The dynamic behaviors that actually govern transitions through multiple conformational states, driven by a hierarchy of strong and weak interactions, are inaccessible using traditional biochemical assays. This knowledge

Significance

Replication of genomic DNA is essential to all cells. The replisome, the multiprotein machine that performs DNA replication, contains many moving parts, the actions of which are poorly understood. Unraveling the dynamic behavior of these proteins requires novel application of single-molecule imaging techniques to eliminate averaging inherent in ensemble methods and to directly observe short-lived events. Here, we present single-molecule observations of an active *Saccharomyces cerevisiae* replisome using purified proteins. We find that a checkpoint complex (Mrc1–Tof1–Csm3), known to bind and to speed up the replisome, interacts only transiently with the replisome. This work represents a major step toward establishing the tools needed to understand the detailed kinetics of proteins within the complex eukaryotic replisome.

Author contributions: J.S.L., L.M.S., G.D.S., R.E.G., M.E.O., and A.M.v.O. designed research; J.S.L., L.M.S., and G.D.S. performed research; G.D.S., F.R.H., R.E.G., and M.E.O. contributed new reagents/analytic tools; J.S.L., L.M.S., G.D.S., M.E.O., and A.M.v.O. analyzed data; and J.S.L., L.M.S., G.D.S., M.E.O., and A.M.v.O. wrote the paper.

Reviewers: D.R., Imperial College London; and M.T., Baylor University.

The authors declare no conflict of interest.

[1]J.S.L. and L.M.S. contributed equally to this work.

[2]To whom correspondence may be addressed. Email: odonnel@rockefeller.edu or vanoijen@uow.edu.au.

This article contains supporting information online at www.pnas.org/lookup/suppl/doi:10.1073/pnas.1711291114/-/DCSupplemental.

is essential to understand these processes in biophysical detail. Single-molecule-based approaches of DNA replication allow real-time observation of individual replisomes, revealing rare intermediates and often surprising dynamics during replication that cannot be otherwise detected (15–17).

Here, we use single-molecule tethered-bead assays to study the kinetics of the leading-strand replisome of a eukaryote, which has replication machinery homologous to that used in humans. The minimal replisome system is reconstituted from the helicase complex Cdc45, MCM2–7, GINS (CMG), the leading-strand DNA Pol ε, the clamp loader Replication Factor C (RFC), the sliding clamp proliferating cell nuclear antigen (PCNA), and ssDNA binding protein (SSB). In the current paper we observe synthesis of the leading strand in real time at rates consistent with cellular observations. In the presence of Minichromosome maintenance protein 10 (Mcm10), we observe a threefold increase in the number of productive replication events and an increase in the basal rate of the minimal replisome, supporting the role of Mcm10 in fork rate and stability after origin firing (6). Mrc1 forms a complex with Tof1 and Csm3, referred to as the MTC fork protection complex. The MTC complex is generally thought to function when the replication fork is challenged with DNA damage or at replication fork barriers (8, 9, 18). In the presence of MTC we observe significantly increased rates of replication, consistent with values previously published (5), and observations that MTC regulates fork speed in the cell (13). Unexpectedly, the MTC complex causes multiple changes in rate over time during a single leading-strand replication reaction observed at the single-molecule level. In sum, the observations documented herein show a highly dynamic interaction between MTC and the leading-strand replisome.

Results

Single-Molecule Visualization of Leading-Strand Synthesis. We use a single-molecule tethered-bead flow-stretching assay (19, 20) to directly visualize the replication kinetics of individual *S. cerevisiae* leading-strand replisomes. A linear and double-stranded DNA substrate (Fig. S1) containing a replication fork is attached to a microbead on one end and the surface of a microscope coverslip on the other (Fig. 1*C*). We apply a laminar flow to exert a controllable drag force on the beads, and thus stretch out the DNA molecules. We use ultrawide-field, low-magnification microscopy to image thousands of beads and relate bead movement to changes in DNA length (17) (Fig. 1 *A* and *B*). At drag forces lower than 6 pN, ssDNA is approximately six times shorter than dsDNA (19, 21). Movement of the bead against the direction of flow, therefore, reports on the conversion from dsDNA to ssDNA. With leading-strand synthesis effectively converting parental DNA into ssDNA on the lagging strand, we can now monitor leading-strand synthesis by a gradual shortening of individual DNA molecules. Topoisomerase is not required because the DNA is free to rotate at both ends, thus preventing accumulation of supercoils. Automated fitting of the bead images and tracking of the bead positions as a function of time provides a readout for these interconversions with high precision (~50 nm, corresponding to ~200 bp) (17). Simultaneously tracking thousands of beads enables high data throughput and the characterizations of subpopulations within individual experiments. We can characterize properties of individual replisomes such as rate (and changes therein) and the product length (the total number of nucleotides synthesized per replisome during the experiment).

To recapitulate previous in vitro (2) results at the single-molecule level, we visualized leading-strand DNA synthesis using the single-molecule tethered-bead flow-stretching assay (Fig. 1*D*). The biotinylated fork is tethered to the streptavidin-coated surface of the flow cell and the digoxigenin couples to a 2.8-μm antidigoxigenin-coated bead (*Materials and Methods*). The leading-strand arm of the

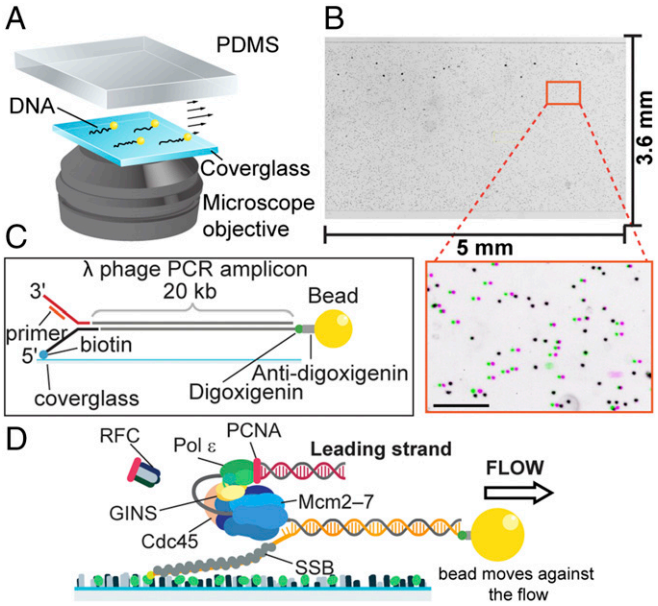

Fig. 1. Single-molecule tethered-bead DNA-stretching assay. (*A*) Experimental setup. DNA molecules are tethered in a microfluidic flow cell. Beads attached to DNA ends are imaged with wide-field optical microscopy. DNA molecules are stretched by applying a laminar flow of buffer. (*B*) A representative field of view showing 4,000 beads. (*Inset*) Image of beads attached to DNA flow-stretched in one direction (magenta) superimposed with an image of the same bead-attached DNA molecules stretched in the opposite direction (green) shows the presence of a large number of DNA-bead tethers. The beads that are improperly tethered are shown in black. (Scale bar, 150 μm.) (*C*) DNA template. A replication fork was introduced at one end of a 20-kb linear substrate, with a bead attachment site at the other end. The fork is attached to the surface via a biotin on the 5′ tail. (*D*) Schematic of leading-strand replication by the minimal *S. cerevisiae* replisome. As dsDNA is converted into ssDNA, the DNA shortens and the bead moves against the direction of flow.

fork contains a 3′ ssDNA tail that is exposed to the solution to facilitate loading of CMG helicase.

Measuring the length difference between ssDNA and dsDNA provides a ratio between the number of processed nucleotides by the DNA polymerase and the amount of observed shortening. Due to the presence of ssDNA binding protein the measured contour length of ssDNA will be higher than that for naked ssDNA. To correct for this difference, we measured the change in ssDNA length upon RPA binding and the ratio was derived between the lengths of dsDNA and RPA-coated ssDNA (Fig. S2). This value was 106 ± 10%, making RPA-coated ssDNA almost the same length as dsDNA. RPA is therefore incompatible with the visualization of changes in DNA length during leading-strand synthesis. Consequently, we used *Escherichia coli* SSB in all replication assays, as ssDNA coated with SSB has a contour length that is 24 ± 2% that of dsDNA, corresponding to an experimental conversion factor of 5,596 ± 73 nt/μm (Fig. S2). *E. coli* SSB and *S. cerevisiae* RPA give indistinguishable results in the leading-strand synthesis reaction (Fig. S3).

Single-Molecule Replication Rates of Pol ε-Dependent Leading-Strand Synthesis. The experimental strategy for establishing the leading-strand replisome is outlined in Fig. 1*D*. First, CMG is loaded onto the fork under a flow of buffer. Subsequently, leading-strand synthesis is initiated by introducing a flow of buffer containing CMG, Pol ε, PCNA, RFC, PCNA, Mg^{2+}, all four dNTPs, and ATP (see *Materials and Methods* for precise details). Fig. 2*A* shows length changes of two individual DNA molecules as a function of time. A gradual shortening of the DNA is clearly visible, indicating sustained conversion of dsDNA into ssDNA.

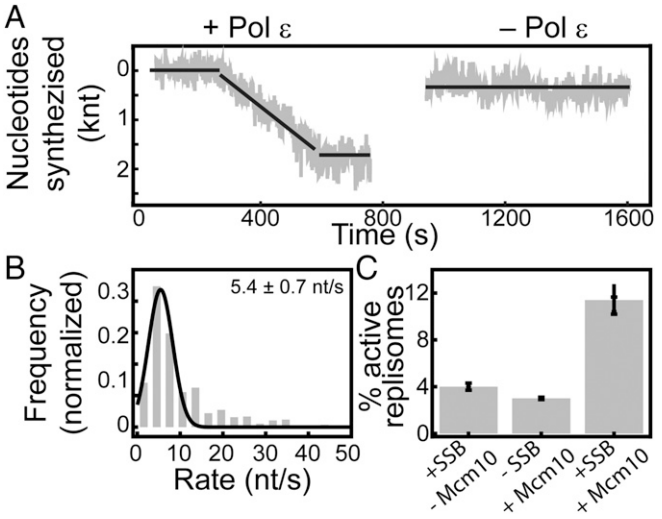

Fig. 2. Single-molecule visualization of leading-strand synthesis by *S. cerevisiae*. (*A*) Representative trajectory showing Pol ε-dependent leading-strand synthesis (left). When Pol ε is omitted no replication events are observed (right). The black lines represent the rate segments identified by the change-point algorithm. (*B*) Histogram of the instantaneous single-molecule rates. The black line represents a Gaussian fit with a rate of 5.4 ± 0.7 nt/s (mean ± SEM) (n = 161 trajectories). (*C*) Efficiencies of leading-strand synthesis, defined as the number of beads that show replication events over the total number of correctly tethered beads. The efficiency is approximately threefold higher (11.4 ± 0.2%, n = 3 experiments) in the presence of SSB and Mcm10, compared with experiments without Mcm10 (4.0 ± 0.3%, n = 4 experiments) or without SSB (3.0 ± 0.1%, n = 2 experiments). The errors represent the experimental error.

To detect rate changes and to identify different operational modes of the leading-strand replisome, we used an unbiased, multiline-fitting algorithm based on change-point theory (17, 22) (Fig. 2*A*, black lines). The rates obtained from this algorithm are weighted by the DNA segment length, reflecting the number of nucleotides that were synthesized at this rate. This places more significance on the longer rate segments, as they have a higher signal-to-noise ratio compared with shorter ones. The rate was determined by fitting the rate histogram with a Gaussian function, resulting in a rate of 5.4 ± 0.7 nt/s (mean ± SEM) (Fig. 2*B*), consistent with earlier ensemble reactions using ^{32}P-dNTPs (2). The rate values in these single-molecule experiments are consistent with previously reported ensemble experiments (1, 2) and use of yeast extracts in single-molecule experiments (23). Instead of using processivity, a term that is ambiguous in definition when comparing experiments with very different protein and DNA concentrations, we leverage the precise nature of our single-molecule measurements to define the product length of individual DNA products. The overall product length for an experiment is determined by measuring the total amount of dsDNA converted into ssDNA for every trajectory and fitting their distribution with a single-exponential decay (assuming a single rate-limiting step determining the end of an event). The product length of Pol ε-dependent leading-strand synthesis was measured to be 0.9 ± 0.2 kilonucleotides (knt) in the 20-min observation time (Fig. S4*A*). These values for a minimal leading-strand replisome are consistent with previously reported ensemble experiments (1, 2). In the absence of the four dNTPs no replication events were observed, demonstrating that the observed bead movements are enzyme-dependent. We note that previous ensemble assays of recombinant CMG show that CMG binds DNA for up to 1 h, and that these longer time windows enable CMGE–PCNA to eventually complete synthesis of a 3-kb template (1–3). In our current setup, however, the typical observation time is 20 min, and we cannot directly observe when enzyme binding and/or unbinding occurs. The processivity/stability of these components on DNA and proficiency to exchange with components from solution should be studied in the future.

To exclude the possibility of Pol ε-independent unwinding of dsDNA by CMG, we performed the experiment in the absence of Pol ε. As expected, we do not see any replication events (Fig. 2*A*). We also performed the experiment lacking CMG but detect no replication events, consistent with inability of Pol ε to strand-displace. Combining these results, we conclude that the effective shortening of the DNA substrate arises from CMG–Pol ε-dependent leading-strand synthesis. This observation provides us with the ability to monitor leading-strand replication of *S. cerevisiae* in real time at the single-molecule level. Additionally, it affords us the opportunity to characterize interactions between proteins within the leading-strand replisome, one replisome at a time.

Mcm10 Increases the Number of Productive Replication Events. Mcm10 has been identified as an important player in CMG activation (24, 25) and maintenance of the replication fork (26). Studies using reconstituted purified proteins have demonstrated that Mcm10 is not absolutely required for leading/lagging strand fork function in vitro (1). To understand the effect of Mcm10 during leading-strand replication at the single-molecule level, we added equimolar amounts of CMG and Mcm10 during initial CMG loading and in the subsequent replication reaction. The addition of Mcm10 did not result in any Pol ε-independent unwinding of dsDNA by CMG. However, addition of Mcm10 to the leading-strand replication reaction resulted in an average of 1.3-fold increase in rate (11.0 ± 0.6 nt/s, Fig. 3*B*), consistent with previous ensemble observations (6). Interestingly, we noticed a significant approximately threefold increase in the number of trajectories that show replication events (Fig. 2*C*). The efficiency is defined as a percentage of the number of correctly tethered beads that show replication. The average number of correctly tethered beads is

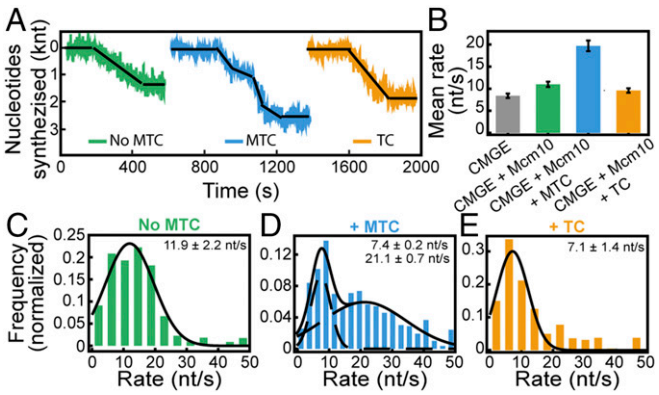

Fig. 3. Effect of MTC on replication kinetics. (*A*) Representative trajectories showing Pol ε-dependent leading-strand synthesis without MTC (left, green), with MTC (middle, blue), and with TC (right, orange). The black lines represent rate segments identified by the change-point algorithm. (*B*) Average single-molecule rates (mean ± SEM) of all segments determined by the change-point algorithm, using CMGE (8.4 ± 0.5 nt/s), CMGE + Mcm10 (11.0 ± 0.6 nt/s), CMGE + Mcm10 + MTC (19.7 ± 1.2 nt/s), and CMGE + Mcm10 + TC (9.6 ± 0.5 nt/s). (*C*) Histogram of the instantaneous single-molecule rates for CMGE + Mcm10. The black line represents a Gaussian fit with a mean rate of 11.9 ± 2.2 nt/s, similar to the rates obtained without Mcm10 (Fig. 2*B*) (n = 96 trajectories). (*D*) Histogram of the instantaneous single-molecule rates for CMGE + Mcm10 + MTC. The histogram shows a bimodal distribution and was fit with the sum of two Gaussian distributions (black line), resulting in rates of 7.4 ± 0.2 nt/s and 21.1 ± 0.7 nt/s (n = 225 trajectories). (*E*) Histogram of the instantaneous single-molecule rates for replication by CMGE + Mcm10 + TC (omitting Mrc1). The fast population associated with MTC activity is not present (n = 111 trajectories).

981 ± 147 (n = 5 experiments). This increase in efficiency suggests that Mcm10 facilitates the assembly of an active leading-strand complex, or enhances its stability as observed earlier (6). Consequently, all further single-molecule experiments included Mcm10.

Addition of MTC Increases Replication Rates of Pol ε-Dependent Leading-Strand Synthesis. Previous studies demonstrated that MTC is required for maximal fork speed in vivo (10, 12, 13) and in vitro (5). The in vitro ensemble experiments, however, did not inform on the lifetime of MTC binding to a leading-strand replisome or on its effect on the instantaneous replication rates. The Mrc1, Tof1, and Csm3 proteins are present in the RPC in a substoichiometric fashion, suggesting they are not present in every replisome or only transiently associated (8). To provide access to this important kinetic information, we repeated the tethered-bead assay in the presence of 30 nM MTC (Fig. 3*A*). We observe a twofold increase in average replication rate (19.7 ± 1.2 nt/s) in the presence of MTC consistent with in vivo observations of fork speed in the presence and absence of Mrc1 (Fig. 3*B*), and an increase in product length (compare Fig. S4*B* with Fig. S4*C*). The overall 1.8-fold rate increase is consistent with several in vivo studies of Mrc1-deficient cells (10–12). Previous work reported that Mrc1 is responsible for the increased fork speed, even though the interaction of MTC with the replisome is largely mediated by Tof1, and that Mrc1 function is largely aided by the presence of Tof1 (5, 8, 12, 13, 18). Consistent with this observation, the increase in leading-strand fork speed we observe requires MTC and is not observed using only the (Tof1–Csm3) TC complex. Leading-strand replication performed in the presence of the TC complex resulted in the loss of the higher rates and loss of the increase in product length compared with the MTC complex that includes Mrc1 (Fig. 3 *B* and *E* and Fig. S4*D*).

MTC Induces Multiple Rate Changes Within a Single Leading-Strand Replication Complex. The single-molecule rate distribution for MTC-mediated leading-strand synthesis shows a bimodal rate distribution, composed of a slow population with a rate of 7.4 ± 0.2 nt/s (mean ± SEM) and a fast population with a rate of 21.1 ± 0.7 nt/s. While these observations appear to suggest an unsaturated reaction, we have titrated MTC into bulk assays from 0 to 120 nM MTC and observe saturation at 15 nM, less than the 30 nM MTC used in the experiments of this paper (Fig. S5). The appearance of these two populations highlights the importance of using single-molecule techniques, as this bimodal distribution would not be visible in traditional ensemble-averaging assays. This bimodal distribution can be explained by two possible mechanisms—one in which MTC speeds up a subset of replisomes or one in which MTC interacts with all replisomes, but only transiently. If the first mechanism were true, a subset of trajectories would exhibit faster rates consistent with these replisomes associated with MTC, whereas the rest would exhibit the slow rate observed in the absence of MTC. If the second mechanism were true, we should see both slow and fast rates within a single trajectory, resulting in multiple rate changes per replisome. To distinguish between these two possibilities, we first quantified the number of rate changes for each replisome. Rate changes were defined by the change-point line-fitting analysis (Fig. S6). On average we observe 4.5 times more rate changes when MTC is present (Fig. 4*A*). This high frequency of rate changes within individual reactions identifies that MTC interacts with all replisomes, but only transiently.

Furthermore, we examined the distribution of rates associated with individual switches between rates. We did so by plotting the rate of a change-point segment within a single-molecule trace, versus the rate of the previous change-point segment in the same trajectory (Fig. 4*B*). The points in this transition plot represent rate pairs from trajectories with multiple rate changes. While we do observe some rate changes in the absence of MTC (Fig. 4*B*, *Top*), the points in the transition plot are clustered close to the diagonal. This clustering indicates that the rate changes are only

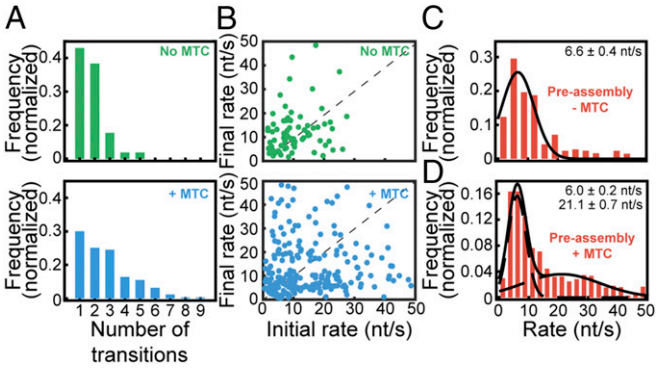

Fig. 4. MTC interaction with the replisome is transient. (*A*) The number of rate changes per trajectory without MTC (*Top*) is 4.5 times lower than with MTC present (*Bottom*). (*B*) Transition plots showing the rate of a segment as a function of the rate of the previous segment for trajectories with multiple segments, with (*Top*) and without (*Bottom*) MTC. The distance from the diagonal (dashed line) is ~2.5-fold higher with MTC (13.6 ± 1.1 nt/s, mean ± SEM) than without MTC (5.9 ± 0.6 nt/s, mean ± SEM). (*C*) Histogram of the instantaneous single-molecule rates obtained with MTC present during loading but omitted from the replication phase. The rate is 6.6 ± 0.4 nt/s, similar to the rates obtained in our continuous flow experiments without MTC. No MTC-mediated fast-rate population was observed (n = 101 trajectories). (*D*) Histogram of the instantaneous single-molecule rates obtained from an experiment where Pol ε was present during loading but omitted from the replication phase. In contrast to the experiment in *C*, the faster population is present. Fitting with the sum of two Gaussians gives rates of 6.0 ± 0.2 nt/s and 21.1 ± 0.7 nt/s (n = 196 trajectories).

minor and are probably due to the small intrinsic rate variations of Pol ε-dependent synthesis. In contrast, when MTC is present the points in the transition plot lie much further away from the diagonal (Fig. 4*B*, *Bottom*). This deviation from the diagonal shows that the change in the rate between two segments in a single trajectory is large. These large changes imply that the replisome can transition from fast, MTC-mediated rates to the slow rates, and vice versa. To quantify the average change in rate between transitions within a single trajectory, we calculated the average distance from the diagonal for all of the points in the transition plot. In the presence of MTC the average rate change is ~2.5-fold higher with a rate change of 13.6 ± 1.1 nt/s (mean ± SEM) compared with 5.9 ± 0.6 nt/s in the absence of MTC. Moreover, the fact that the off-diagonal points are symmetrically distributed around the diagonal illustrates that it is just as likely for a slow rate segment to be followed by a fast rate segment as it is for a fast rate segment to be followed by a slow one. This lack of bias reveals that MTC can bind and unbind from the replisome after replication has started. This observation further supports that MTC undergoes cycles of binding to the replisome from solution, and dissociation. We verified that placing the 3XFLAG tag on the C terminus of Mrc1 and no tag on Csm3 within MTC instead of the N-terminal FLAG–Mrc1 (i.e., compared with use of a C-terminal FLAG tag on Mrc1 and a C-terminal calmodulin tag on Csm3 in refs. 5 and 7) did not result in appreciable differences in the ability of MTC to induce multiple rate changes within single leading-strand replication complexes (Fig. S7).

MTC Is Transiently Associated to the CMGE Leading-Strand Replication Fork Complex. We reasoned that if MTC is indeed weakly bound to the replisome we should be able to decrease the frequency of rate transitions by lowering the concentration of MTC. Replication reactions performed in the presence of either 10 nM or 3 nM MTC showed a reduction in the number of fast rates as well as the frequency of transitions within a single trajectory (Fig. S8). To extend these observations, we performed leading-strand synthesis under conditions permitting preassembly of replisomes at the fork. If

indeed MTC transiently associates with the replisome, we should not see the faster rates when we include MTC during the assembly phase, but omit it from the subsequent replication reaction, as it would dissociate by the time the replication reaction started. As predicted, the rate distribution did not show the fast population (Fig. 4*C*). In contrast, when the CMGE complex is assembled on DNA and Pol ε is omitted from the subsequent replication reaction but MTC is present in the buffer flow the faster population is evident (Fig. 4*D*). This result indicates that Pol ε remains stably bound to the replisome, consistent with previous reports (3). Combining these results, we hypothesize that MTC has a weak affinity for the leading-strand replisome and interacts in a dynamic fashion to increase the rate of the replication fork.

Discussion

We have used a DNA-stretching assay to visualize in vitro leading-strand synthesis by the *S. cerevisiae* replisome at the single-molecule level. Similar experiments have been reported for the T7 and *E. coli* replisomes (17, 20, 27, 28), but a detailed kinetic analysis of the eukaryotic replisome at the single-molecule level has been unavailable thus far. The leading-strand synthesis rates observed here are similar to those previously reported in ensemble biochemical reactions (1, 5) and within the range of replication fork movement observed inside the cell (12, 29, 30). This assay has allowed us to probe the effect of Mcm10 and MTC on leading-strand replisome activity, confirming reports that Mcm10 stimulates the minimal replisome in the absence of MTC (6), and that MTC stimulates the replisome rate by an average of 1.8-fold, as summarized in Fig. 5. The observations of Mrc1-dependent stimulation of fork rate are also consistent with cell biology studies of fork movement in Mrc1 cells (10–12). Interestingly, observation at the single-molecule level has revealed unexpected kinetic behaviors that would have been impossible to observe with conventional biochemical assays.

We observe that Mcm10 does not substantially increase the rate or product length of leading-strand synthesis but does increase the number of productive replication events, consistent with a recent study indicating that Mcm10 stabilizes the CMG on DNA (6). This Mcm10-associated increase in efficiency could be relevant to the conclusions that Mcm10 functions as an activator of the CMG complex throughout DNA replication (6, 31), assisting stabilization of CMG or helping it overcome possible obstacles. Mcm10 is also known to activate Mcm2–7 during replication initiation (24, 32, 33). It is conceivable that Mcm10 helps activate Mcm2–7 in our in vitro leading-strand system through a similar mechanism. It also remains possible that Mcm10 stabilizes Pol ε or otherwise enhances its synthesis activity.

The current study demonstrates that the MTC complex increases the rate of leading-strand synthesis in an unexpected fashion (summarized in Fig. 5*C*). The MTC complex appears to act in a highly dynamic fashion, only transiently active at the replisome. This observation is consistent with the substoichiometric presence of these subunits in the RPC complex (34). We observe processive leading-strand reactions at the single-molecule level with short-lived phases of higher rates that we interpret as corresponding to MTC binding to the replisome. Interestingly, the instantaneous rates during these phases increase by threefold but average out to an approximately twofold average rate increase because they do not persist throughout the entire trajectory of an individual replisome. Further, the twofold average rate increase is consistent with observations of Mrc1 in the cellular context (10–12). The fluctuating rates per single-molecule trajectory suggest that MTC is distributive and does not bind to the replisome in a stable manner. Distributive behavior of critical replisome components has precedent in bacterial DnaG primase (35). When we compare the rates of successive segments within one trajectory we see that fast MTC-mediated rates can be followed by slow rates, and vice versa. Furthermore, the amplitude of these rate changes is on average ∼2.5-fold higher than the rate changes without MTC. This observation demonstrates that MTC or one of its components (e.g., Mrc1) associates with and dissociates from the replisome multiple times during leading-strand synthesis. The fact that we do not observe any fast rates when MTC is omitted during the replication phase, but is present during the CMG loading phase of a preassembly experiment, further supports the conclusion that transient interactions exist between MTC and the replisome. These data contrast with previous models that suggest that Mrc1 stably binds to both CMG and Pol ε (8), though we note that cross-linking in ChIP assays prevents dynamics, and pulldowns are not quantitative. It was proposed that this pair of interactions could be responsible for the faster rates, by tethering Pol ε to CMG (13, 36). The higher kinetic resolution of our experiments reveals the dynamic interaction of MTC with the replisome, with the population-averaged observables consistent with earlier biochemical assays. From the current study, however, we cannot conclude whether MTC acts to stimulate the DNA polymerase or the rate of unwinding, or both.

It is important to note that the exact phosphorylation state of the proteins is expected to play a role in MTC–replisome interactions (37). In addition, the current study focuses on the enzymes of leading-strand synthesis while additional proteins could play a role in MTC behavior. Replication proteins in *S. cerevisiae* undergo many posttranslational modifications before and during replication (38, 39). For example, Dbf4-dependent kinase (DDK) and cyclin-dependent kinase (CDK) are known to control replication initiation by phosphorylation of many proteins involved in forming the origin recognition complex (39, 40). Additionally, phosphorylation of replisome components plays an important role in programmed fork arrest through phosphorylation of Mcm2–7, which promotes recruitment of Tof1–Csm3 by the replisome (37). *S. cerevisiae* recombinant expressed CMG and Tof1–Csm3 are phosphoproteins that facilitate their interaction (37). Interestingly, upon coexpression of CMG the vast majority of expressed proteins are free Mcm2–7, Cdc45 and GINS that do not simply self-assemble into a CMG complex (40). Thus, it is possible that the small amount of recombinant CMG recovered from expression cells is in fact assembled at origins (2). We note that Mrc1 has previously been shown to be the only component of MTC that enhances replisome rate (5), and since our observations rely on the conversion of dsDNA to ssDNA it is possible that the dynamic interactions reported herein are of Mrc1 instead of the entire MTC complex.

It is tempting to speculate a possible biological reason for a dynamic interaction of Mrc1/MTC with the replisome. We presume that the different replication rates that correspond to the association state of Mrc1/MTC reflect different conformations of the replisome. Different replisome conformations may in turn facilitate active-site configurations (i.e., enzymatic velocities), additional protein interactions, or exchange with other partners, in a differential manner. An interesting aspect of MTC activity is its

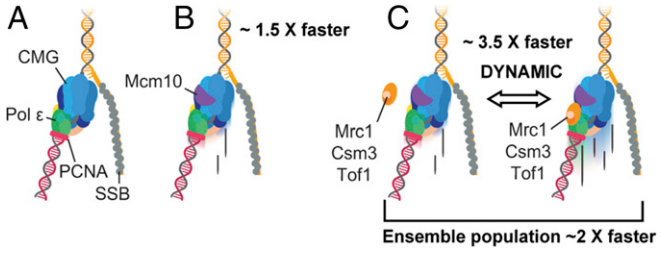

Fig. 5. Leading-strand synthesis by the *S. cerevisiae* replisome. (*A*) The minimal reconstituted leading-strand replisome supports leading-strand synthesis at a rate of 5.4 ± 0.7 nt/s. (*B*) Addition of Mcm10 increases the rate ∼1.5 fold (11.9 ± 2.2 nt/s). (*C*) The MTC complex speeds up the leading-strand replisome by ∼3.5 fold. Our single-molecule measurements demonstrate that MTC has a weak affinity for the replisome and only transiently interacts to speed up replication.

phosphorylation state. For example, it is well known that Mrc1 mediates the DNA-damage response through phosphorylation of Mrc1 by the Mec1/Rad53 kinases (41). The advantage of a dynamic interaction of Mrc1/MTC with CMG could provide an interesting type of regulation. The dynamic interaction between MTC and the replisome documented herein could ensure a complete sampling of the phosphorylation state of MTC by all replisomes, as opposed to only a subset of replisomes carrying a fully phosphorylated MTC complex. A dynamic mechanism of MTC–replisome interaction would allow the MTC to act as a potentiometer for damage. The ratio of modified and unmodified MTC (i.e., in response to DNA damage) would be "sensed" by all replisomes equally, instead of a stark division in the case of a stable interaction of MTC with CMG, which would result in different fork speeds within the same cell. Hence, a dynamic interaction would provide a gradual titration of phosphorylated MTC, equally sampled by all replisomes, and consequently provide a more uniform fork speed. Despite these studies revealing the dynamic nature of MTC within a replisome, future studies are required to understand how replication proteins interact in vitro and in living cells.

Materials and Methods

Protein Expression and Purification. CMG, Pol ε, RFC, PCNA, RPA, and SSB were purified as described (2). Purification of Mcm10 and MTC (Fig. S9) is described in *Supporting Information*.

Linear Fork DNA Substrates. DNA replication templates used in ensemble leading-strand experiments were prepared as described (2, 14). The replication substrate used for surface tethering and bead attachment in single-molecule experiments was constructed using a 19,979-bp PCR λ-phage product and the HPLC purified oligonucleotides listed in Table S1 (Integrated DNA Technologies). See *Replication Assays* for full details.

Single-Molecule Tethered-Bead Assay. Flow cells were prepared as described (17, 42). First, CMG was loaded at the fork using 30 nM CMG, 30 nM Mcm10, and MTC (where indicated) in replication buffer [25 mM Tris·HCl, pH 7.6, 10 mM Mg acetate, 50 mM K glutamate, 40 μg/mL BSA, 0.1 mM EDTA, 5 mM DTT, and 0.0025% (vol/vol) Tween-20] at 15 μL/min for 10 min. Reactions were initiated by introducing 30 nM CMG, 30 nM Mcm10, 40 nM Pol ε, 20 nM PCNA, 6 nM RFC, 250 nM *E. coli* SSB, and MTC (where indicated) in replication buffer supplemented with 5 mM ATP and 60 μM dCTP, dGTP, dATP, and dTTP. See *Replication Assays* for full details.

Ensemble Leading-Strand Replication Assays. Replication reactions (25 μL) contained 25 mM Tris-acetate, pH 7.5, 5% (vol/vol) glycerol, 40 μg/mL BSA, 3 mM DTT 2 mM Tris(2-carboxyethyl)phosphine, 10 mM Mg acetate, 50 mM K glutamate, 0.1 mM EDTA, 5 mM ATP, and 120 μM of each dNTP unless otherwise noted. See *Replication Assays* for full details.

Code Availability. Source code for most analysis tools is available at GitHub under Single-Molecule Biophysics beadpy, or upon request.

ACKNOWLEDGMENTS. We thank Olga Yurieva and Dan Zhang for MTC, Pol ε, CMG, and Mcm10 and Karl Duderstadt for single-molecule analysis software. This work was supported by Australian Research Council Grant DP150100956, Australian Laureate Fellowship FL140100027 (to A.M.v.O.), Fundamenteel onderzoek der materie Grant 12CMCE03 (to L.M.S.), NIH Grant GM-115809 (to G.D.S. and M.E.O.), and Howard Hughes Medical Institute (G.D.S. and M.E.O.).

1. Georgescu RE, et al. (2015) Reconstitution of a eukaryotic replisome reveals suppression mechanisms that define leading/lagging strand operation. *Elife* 4:e04988.
2. Georgescu RE, et al. (2014) Mechanism of asymmetric polymerase assembly at the eukaryotic replication fork. *Nat Struct Mol Biol* 21:664–670.
3. Langston LD, et al. (2014) CMG helicase and DNA polymerase ε form a functional 15-subunit holoenzyme for eukaryotic leading-strand DNA replication. *Proc Natl Acad Sci USA* 111:15390–15395.
4. Devbhandari S, Jiang J, Kumar C, Whitehouse I, Remus D (2017) Chromatin constrains the initiation and elongation of DNA replication. *Mol Cell* 65:131–141.
5. Yeeles JTP, Janska A, Early A, Diffley JFX (2017) How the eukaryotic replisome achieves rapid and efficient DNA replication. *Mol Cell* 65:105–116.
6. Lõoke M, Maloney MF, Bell SP (2017) Mcm10 regulates DNA replication elongation by stimulating the CMG replicative helicase. *Genes Dev* 31:291–305.
7. Kurat CF, Yeeles JTP, Patel H, Early A, Diffley JFX (2017) Chromatin controls DNA replication origin selection, lagging-strand synthesis, and replication fork rates. *Mol Cell* 65:117–130.
8. Katou Y, et al. (2003) S-phase checkpoint proteins Tof1 and Mrc1 form a stable replication-pausing complex. *Nature* 424:1078–1083.
9. Alcasabas AA, et al. (2001) Mrc1 transduces signals of DNA replication stress to activate Rad53. *Nat Cell Biol* 3:958–965.
10. Tourriere H, Versini G, Cordon-Preciado V, Alabert C, Pasero P (2005) Mrc1 and Tof1 promote replication fork progression and recovery independently of Rad53. *Mol Cell* 19:699–706.
11. Szyjka SJ, Viggiani CJ, Aparicio OM (2005) Mrc1 is required for normal progression of replication forks throughout chromatin in S. cerevisiae. *Mol Cell* 19:691–697.
12. Hodgson B, Calzada A, Labib K (2007) Mrc1 and Tof1 regulate DNA replication forks in different ways during normal S phase. *Mol Biol Cell* 18:3894–3902.
13. Lou H, et al. (2008) Mrc1 and DNA polymerase ε function together in linking DNA replication and the S phase checkpoint. *Mol Cell* 32:106–117.
14. Schauer GD, O'Donnell ME (2017) Quality control mechanisms exclude incorrect polymerases from the eukaryotic replication fork. *Proc Natl Acad Sci USA* 114:675–680.
15. Lewis JS, et al. (2017) Single-molecule visualization of fast polymerase turnover in the bacterial replisome. *Elife* 6:e23932.
16. Geertsema HJ, van Oijen AM (2013) A single-molecule view of DNA replication: The dynamic nature of multi-protein complexes revealed. *Curr Opin Struct Biol* 23:788–793.
17. Duderstadt KE, et al. (2016) Simultaneous real-time imaging of leading and lagging strand synthesis reveals the coordination dynamics of single replisomes. *Mol Cell* 64:1035–1047.
18. Bando M, et al. (2009) Csm3, Tof1, and Mrc1 form a heterotrimeric mediator complex that associates with DNA replication forks. *J Biol Chem* 284:34355–34365.
19. van Oijen AM, et al. (2003) Single-molecule kinetics of λ exonuclease reveal base dependence and dynamic disorder. *Science* 301:1235–1238.
20. Lee J-B, et al. (2006) DNA primase acts as a molecular brake in DNA replication. *Nature* 439:621–624.
21. Bustamante C, Marko JF, Siggia ED, Smith S (1994) Entropic elasticity of lambda-phage DNA. *Science* 265:1599–1600.
22. Watkins LP, Yang H (2005) Detection of intensity change points in time-resolved single-molecule measurements. *J Phys Chem B* 109:617–628.
23. Duzdevich D, et al. (2015) The dynamics of eukaryotic replication initiation: Origin specificity, licensing, and firing at the single-molecule level. *Mol Cell* 58:483–494.
24. Perez-Arnaiz P, Bruck I, Kaplan DL (2016) Mcm10 coordinates the timely assembly and activation of the replication fork helicase. *Nucleic Acids Res* 44:315–329.
25. van Deursen F, Sengupta S, De Piccoli G, Sanchez-Diaz A, Labib K (2012) Mcm10 associates with the loaded DNA helicase at replication origins and defines a novel step in its activation. *EMBO J* 31:2195–2206.
26. Bielinsky A-K (2016) Mcm10: The glue at replication forks. *Cell Cycle* 15:3024–3025.
27. Tanner NA, et al. (2008) Single-molecule studies of fork dynamics in *Escherichia coli* DNA replication. *Nat Struct Mol Biol* 15:170–176.
28. Hamdan SM, et al. (2007) Dynamic DNA helicase-DNA polymerase interactions assure processive replication fork movement. *Mol Cell* 27:539–549.
29. Sekedat MD, et al. (2010) GINS motion reveals replication fork progression is remarkably uniform throughout the yeast genome. *Mol Syst Biol* 6:353.
30. Conti C, et al. (2007) Replication fork velocities at adjacent replication origins are coordinately modified during DNA replication in human cells. *Mol Biol Cell* 18:3059–3067.
31. Chadha GS, Gambus A, Gillespie PJ, Blow JJ (2016) Xenopus Mcm10 is a CDK-substrate required for replication fork stability. *Cell Cycle* 15:2183–2195.
32. Quan Y, et al. (2015) Cell-cycle-regulated interaction between Mcm10 and double hexameric Mcm2-7 is required for helicase splitting and activation during S phase. *Cell Rep* 13:2576–2586.
33. Baxley RM, Bielinsky A-K (2017) Mcm10: A dynamic scaffold at eukaryotic replication forks. *Genes (Basel)* 8:E73.
34. Gambus A, et al. (2006) GINS maintains association of Cdc45 with MCM in replisome progression complexes at eukaryotic DNA replication forks. *Nat Cell Biol* 8:358–366.
35. Tougu K, Marians KJ (1996) The interaction between helicase and primase sets the replication fork clock. *J Biol Chem* 271:21398–21405.
36. Labib K (2008) Making connections at DNA replication forks: Mrc1 takes the lead. *Mol Cell* 32:166–168.
37. Bastia D, et al. (2016) Phosphorylation of CMG helicase and Tof1 is required for programmed fork arrest. *Proc Natl Acad Sci USA* 113:E3639–E3648.
38. Siddiqui K, On KF, Diffley JFX (2013) Regulating DNA replication in eukarya. *Cold Spring Harb Perspect Biol* 5:a012930.
39. Bell SP, Labib K (2016) Chromosome duplication in *Saccharomyces cerevisiae*. *Genetics* 203:1027–1067.
40. Bruck I, Dhingra N, Kaplan DL (2017) A positive amplification mechanism involving a kinase and replication initiation factor helps assemble the replication fork helicase. *J Biol Chem* 292:3062–3073.
41. Zhou BB, Elledge SJ (2000) The DNA damage response: Putting checkpoints in perspective. *Nature* 408:433–439.
42. Geertsema HJ, Duderstadt KE, van Oijen AM (2015) Single-molecule observation of prokaryotic DNA replication. *Methods Mol Biol* 1300:219–238.